2D Materials 2.3 (2015): 035008

DOI: http://dx.doi.org/10.1088/2053-1583/2/3/035008

Exfoliated graphite flakes as soft-electrodes for precisely contacting nanoobjects

P Ares[1,5], G López-Polín[1,5], C Hermosa[2], F Zamora[2,3], J Gómez-Herrero[1,3,4] and C Gómez-Navarro[1,3,4]

[1] Departamento de Física de la Materia Condensada, Universidad Autónoma de Madrid, E-28049 Madrid (Spain)
[2] Departamento de Química Inorgánica, Universidad Autónoma de Madrid, E-28049 Madrid (Spain)
[3] Condensed Matter Physics Center (IFIMAC), Universidad Autónoma de Madrid, E-28049 Madrid (Spain)
[4] INC, Spain
E-mail: pablo.ares@uam.es, julio.gomez@uam.es

[5] These authors contributed equally to this work

Abstract
We introduce a simple, clean and reliable method to transfer exfoliated graphite flakes as soft-electrodes for the electrical contact of nano-objects. The microelectrodes thus produced exhibit extremely well-defined and thin edges and can be placed on any sample location with sub-micrometer precision. The procedure is carried out under ambient conditions and does not require chemical agents. We present electrical characterization of relevant examples including carbon nanotubes, metal-organic MMX nanoribbons, reduced graphene sheets and damaged circuit repair. The quality of the electrical contacts thus obtained is as good as those fabricated with conventional techniques. This technique is particularly relevant for conductive atomic force microscopy (AFM) studies.

Keywords: electrical transport, nanoelectronics, exfoliated graphite, soft-electrode transfer, conductive atomic force microscopy

1. Introduction

Nano and molecular electronics are an important source of inspiration for modern science [1, 2]. Electrodes are a basic requirement for any electrical circuit and they very often provide the link between the nano- and the macro-scale [3-5]. The electrical contact resistance between the electrodes and the nano-objects is a quite commom drawback for and adequate understanding of the electrical properties of these nano-objects. Fabricating electrodes for molecular electronics studies typically requires a high number of steps such as metal evaporation in vacuum, lithography and sample cleaning involving chemical agents. Unfortunately, many candidates for conducting molecules, such as organic biomolecules [6-8] and metal-organic wires [9], are contaminated during these procedures; they are damaged when exposed to vacuum, they do not withstand the high temperatures associated with metal evaporation or they are incompatible with the chemical agents used to clean the rest of the lithography masks. A paradigmatic case is

that of DNA molecules where the influence of metal evaporation on the integrity of the molecules has generated great debate [6, 10, 11]. The influence of the evaporated electrodes was thoroughly discussed in a recent paper on DNA conductivity [8]. In addition, the conventional lithography-based methods entail considerable efforts in terms of time and resources that in many cases are not even available in laboratories.

In this work, we introduce a technique based on the transference of microelectrodes [12], in particular 2D materials [13, 14]. In our approach we take advantage of previously described procedures with the aim of fabricating microelectrodes from exfoliated graphite flakes (EGFs) in an easy, inexpensive and reliable way [15]. The as-produced microelectrodes can be placed with sub-micrometer precision on any sample location. The described technique does not require a vacuum or chemical agents; the whole procedure is based on soft-lithography procedures and it is carried out in ambient conditions. The electrodes exhibit extremely well-defined and steep edges, facilitating the measurements of very short channel lengths. The electrical resistance of our electrodes with several conducting nanomaterials is shown to be within the values reported for conventional metal electrodes. The covalent-bond structure of graphite will provide stable electrodes at room temperature and for long periods of time [16]. The transfer process clearly depends on experience of the operator but after a few attempts, it should not take longer than 30-60 minutes.

This work is structured as follows: first we provide a description of the technique and then we present four relevant examples that illustrate the potential of the procedure. The first two examples correspond to 1D molecules (carbon nanotubes and metal organic nanoribbons), where one of the electrodes is based on EGF and the second electrode is a conducting AFM tip (c-AFM). The third example is the electrical characterization of a known 2D material, reduced graphene oxide with two EGF electrodes. In the last example we show how a broken circuit can be repaired by the controlled position of EGF electrodes.

2. Experimental details

A detailed explanation of the procedure for transferring bidimensional materials is provided in reference [13] and its supporting information. Figure 1 summarizes the key elements of the experimental set up for soft-electrode transfer. It comprises a zoom optical microscope, a XY linear stage and a XYZ micro-manipulator. In our case the price for the whole experimental set up was below 3000 euros (in this work we also present images taken with a high resolution optical microscope but this equipment is not essential for soft-electrode transfer).

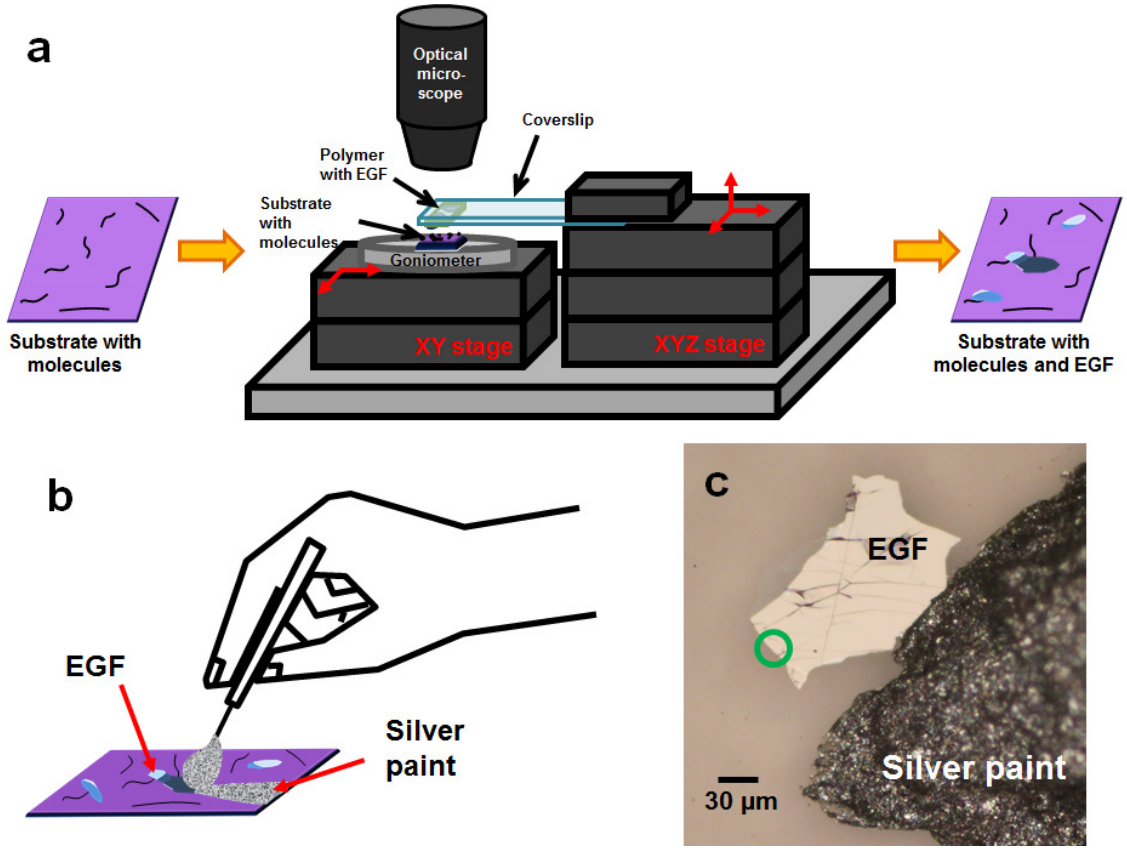

Figure 1. Experimental set up used for soft-electrode transfer. (a) A sample with nano-objects on its surface is placed on the transfer setup consisting on a zoom optical microscope, an XY linear stage and an XYZ manipulator. A viscolestaic polymer is fixed underneath a glass slide held by the XYZ manipulator. The viscoelastic polymer carries exfoliated graphite flakes that are transferred to the substrate by pressing against it. (b) Silver paint is used to create a contact on the selected electrode. (c) Final result where an exfoliated graphite flake and the macroscopic silver paint contact can be readily seen. Green circle encloses an area where carbon nanotubes were previously observed by AFM.

We start by obtaining EGFs from a graphite sample by microexfoliation. The tape containing the flakes is then pressed against a piece of transparent viscoelastic polymer (Gel-Film® from Gel-Pak®) previously fixed to a microscope slide. Importantly, viscoelastic polymers exhibit adhesion that increases with speed. The glass slide is held by a XYZ manipulator. Using the optical microscope we select a convenient EGF. Depending on the application itself the EGF size can vary. For applications where a subsequent macroscopic contact is performed using a conductive paint, at least one of the lateral dimensions needs to be large enough for this handmade contact. This typically implies one of the lateral dimensions to be larger than ~100 µm, however this can be accomplished by grouping several EGFs with increasing sizes. Thus, the smallest lateral dimension should be within optical microscopy resolution. The EGF has to be thick enough to act as a continuous reservoir of electrons without discrete level structure and no gate dependence [16]. Thus we select flakes of ~ 3 to 40 nm thicknesses to fulfil these conditions. Then we place a sample with the nano-objects that we want to contact in the XY linear stage. The sample is observed through the glass slide with the viscoelastic polymer attached to it (figure 1a). By inspecting with the microscope it is possible to locate a suitable

region on the sample and then we move the XYZ manipulator to precisely align the selected EGF on top of the selected sample region. At this point, we lower the polymer pressing hard onto the sample and then we slowly back up. This is the critical point of the procedure; as viscoelastic polymers show a moderate adhesion at low speed, the EGF adheres to the sample surface detaching the polymer. Finally, with the help of the microscope, we create a contact on the selected EGF using a thin brush and silver paint (figures 1b and 1c); this is a distinct an important feature of our procedure. A picture of the experimental set up is also shown in the supporting information (figure S1). A rather similar procedure can be carried out with a thin film of evaporated metal, as for instance gold [17], but as we shall see, the flakes present much more irregular and thicker edges that in some cases might introduce complications. Moreover, since this technique needs previous metal evaporations, it is more time-consuming and requires additional expensive evaporation equipment.

Atomic force microscopy images were acquired with a Nanotec Electrónica SL set up controlled by WSxM software [18]. ElectriMulti75-G Cr/Pt coated probes from BudgetSensors were employed for electrical measurements. Samples were first imaged in non-contact dynamic mode, and then at a selected spot of the nano-object a force vs. distance curve was obtained, and at the maximum tip indentation a current vs. voltage curve was acquired [19]. We have tested a variety of c-AFM probes and experimental conditions yileding similar results.

Probe station measurements were carried out using a home-made two-contact set up that includes a Keithley 2400 sourcemeter, a Keithley 2000 multimeter and a home-made current to voltage preamplifier with selectable gains (ranging from 1 $\mu A\ V^{-1}$ to 1 $nA\ V^{-1}$). Electrical probes are mounted on two independent XYZ micromanipulators.

3. Results and discussion

3.1. Carbon nanotubes

The first example of this work is the electrical contact of carbon nanotubes with EGFs. The procedure is summarized in figure 2. For this purpose a mica substrate with nanotubes on top is prepared by drop casting of a nanotube suspension [20].The concentration of nanotubes is adjusted, with the help of AFM, to be about 1-2 nanotubes every 25 μm^2. First, by using AFM we locate regions with a good density of carbon nanotubes, and then we place an EGF in one of these regions.

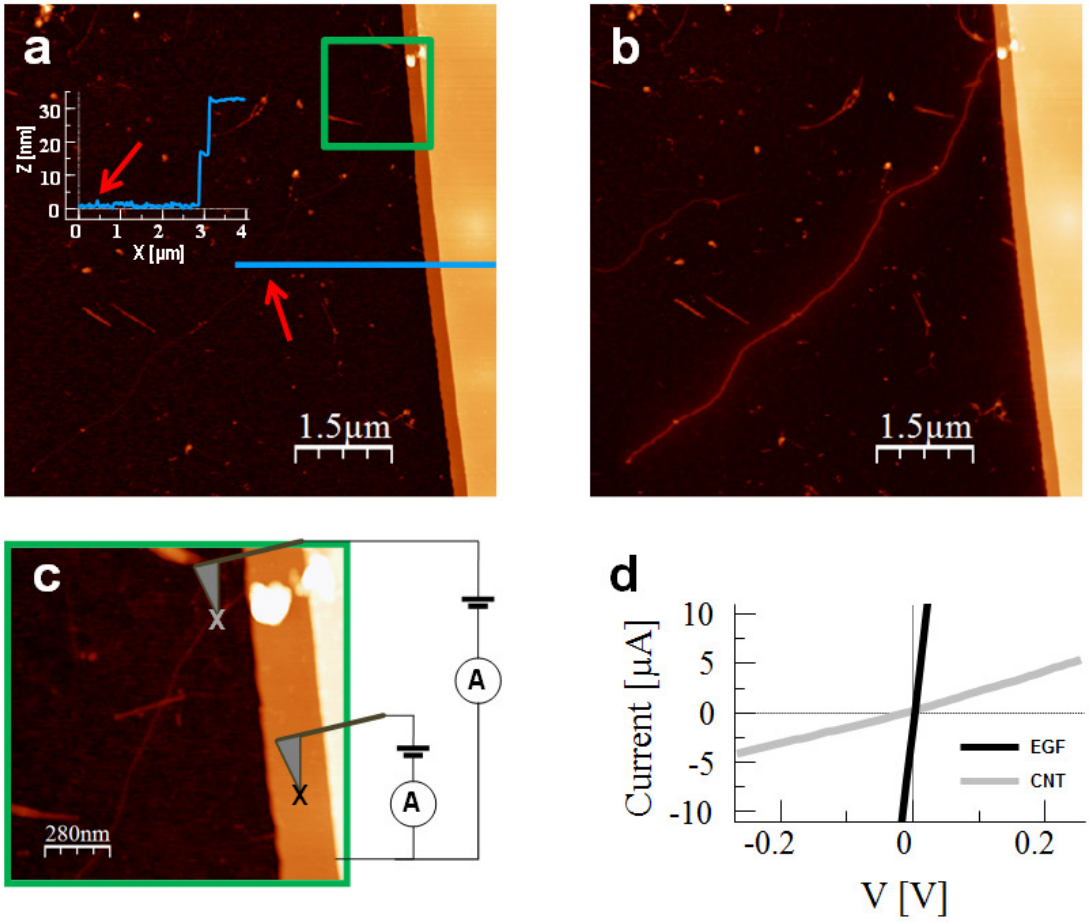

Figure 2. Contacts from carbon nanotubes. (a) AFM topographic image at zero bias voltage in the area enclosed inside the green circle in figure 1c, exhibiting the characteristic sharp edge of the EGF. The inset is a profile along the blue line showing the height of the flake. The red arrows mark the position of the nanotube. (b) Same as (a) but with a 4 V tip-sample bias applied in order to enhance the nanotube contrast. (c) Zoom-in of (a) showing the contact position at which the electrical characterization is carried out (gray and black crosses). Schematics of the electrical circuits at the nanotube and EGF soft-electrode positions are also shown. (d) Current versus voltage characteristics of the nanotube (gray) and electrode (black).

Figure 2a shows an AFM topographic image taken within the green circle shown in figure 1c. The inset shows a profile on the image, where we can measure the height of the lower terrace of the EGF to be ~15 nm. As apparent in both the image and the profile, the flake edge is extremely steep, much steeper than contacts fabricated by thermal evaporation [6]. Besides, there are no traces of contamination or degradation along it. Figure 2b is the same region as in figure 2a but now a tip-sample bias gate of 4 V is applied to enhance the contrast of the nanotube [21, 22]. Figure 2c shows a zoom-in image of the green square drawn in figure 2a. Figure 2c also shows the corresponding schemes for the associated electrical circuits. In brief, a conducting AFM tip is used as a second mobile electrode to measure the current through the nanotube [20]. Figure 2d displays linear current vs. voltage characteristics measured for the nanotube and the EGF (light gray and black crosses in figure 2c). From the slope of the current vs. voltage curve we obtain resistances of 1.7 and 47 kΩ for the flake and the nanotube,

respectively. The resistance measured for the flake by c-AFM is a consequence of the small contact area between the AFM tip and the flake since the resistance of the EGF and the silver paint was found to be below 100 Ω. The resistance measured for the carbon nantotube has contributions from both the contact resistance and the intrinsic resistance of the nanotube, but allows us to have an upper bound of contact resistance of 47 kΩ, which is very similar to that measured with conventional metal electrodes [23, 24]. Please note that previous attempts to contact carbon nanotubes with graphite flakes yielded much higher resistances [15].

3.2. Metal-organic MMX nanoribbons

The next example (summarized in figure 3) describes the use of our procedure to create electrical contacts on platinum-based MMX nanoribbons [25, 26]. Platinum-based MMX polymers are dimetallic subunits with two platinum centres connected by four bridging dithioacetate ligands and an iodine atom bridging the dimetallic units (inset of figure 3a). By direct sublimation of monocrystals of $[Pt_2(dta)_4I]_n$ (*dta*= dithioacetate) on a SiO_2/Si substrate, we are able to form nanoribbons with a high degree of structural perfection. Each nanoribbon is composed of thousands of parallel MMX chains of ~0.8 nm diameter interacting by weak van der Waals forces.

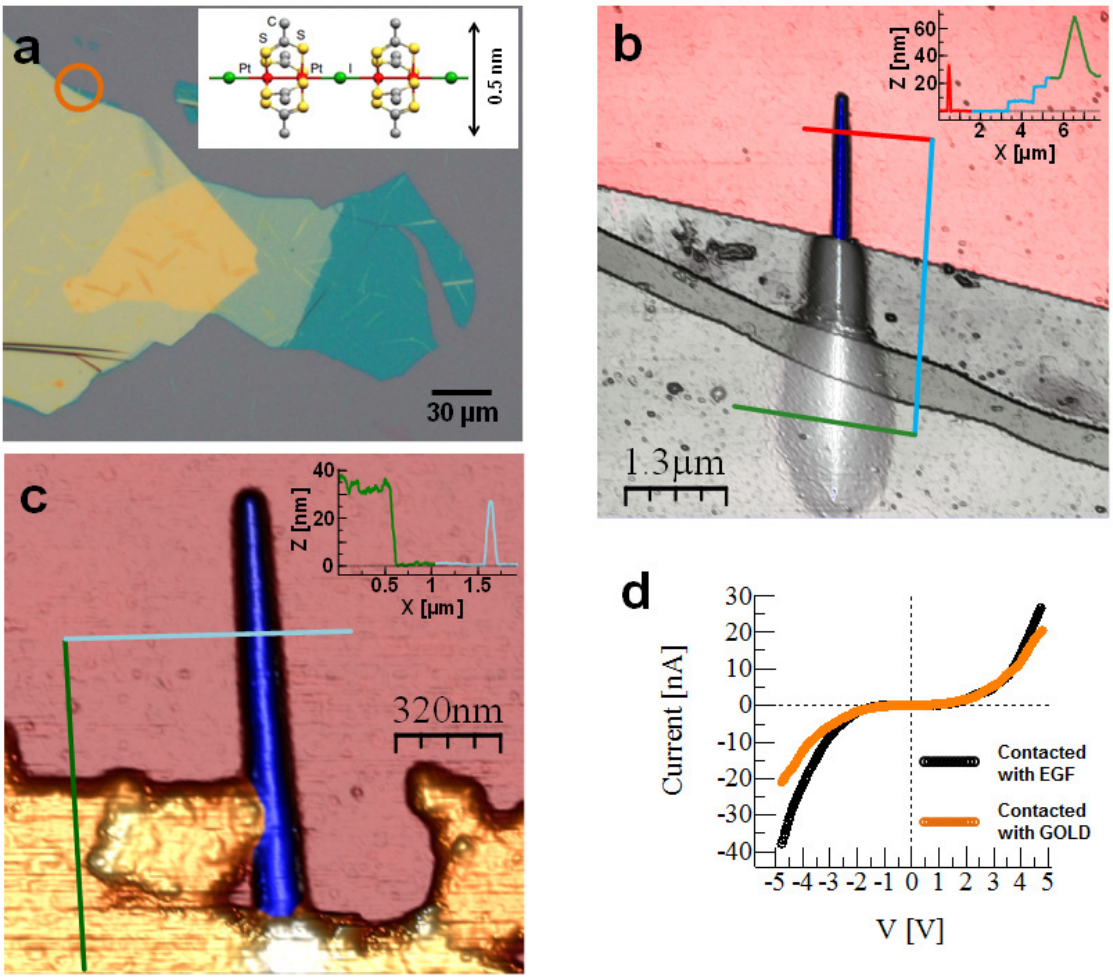

Figure 3. Contacts on MMX nanoribbons. (a) Optical microscope image showing a transferred EGF on a silicon oxide substrate with MMX nanoribbons adsorbed on it. The colors reflect

different flake thicknesses. The thin lines observed below the flakes are ripples caused by the nanoribbons. The inset shows the structure of an individual polymer chain. Every nanoribbon is composed of thousands of these chains. The orange circle enclosures an area with a MMX nanoribbon to be studied by AFM. (b) AFM topographic image of the region within the orange circle in (a). A nanoribbon protruding from the EGF is clearly observed. (c) AFM topographic image of a nanoribbon with a gold flake contact showing typical irregular edges at the nanometer scale. The flake was obtained from a piece of gold thin film transferred in a similar way to the EGF. (d) Current versus voltage characteristics obtained for the nanoribbon with a contact of an EGF (black) and gold (orange).

These MMX polymers are perfect examples of nano-objects based on molecule self-assembly that are very difficult to add contacts by conventional techniques. Similar nanoribbons to the ones used here, but obtained by drop casting cannot withstand the vacuum needed to evaporate conventional metal electrodes: the sudden evaporation of the solvent molecules adsorbed within the ribbons results in a large number of defects along the chains and turns them into electrical insulators [9]. In the present work, we use MMX nanoribbons obtained by sublimation of crystals that do not present this problem. We are currently performing similar work on nanoribbons obtained by drop casting.

To create electrical contacts on the MMX nanoribbons we transfer the EFGs onto SiO_2 substrates with MMX nanoribbons previously deposited. Figure 3a displays an optical microscope image of such a sample. The colours observed in the images reflect different flake thicknesses. The optical image allows us to see nanoribbons covered by the flake. Figure 3b shows an AFM topographic image showing a nanoribbon partially covered by an EGF with a very well-defined edge. According to the inset in this figure, the height of the lower EGF terrace is ~5 nm. MMX nanoribbons with such contacts are tested, as in the previous example, by using a conductive AFM tip as a second mobile electrode. A representative IV curve obtained for one of these nanoribbons is displayed in figure 3d. The conductivity obtained for these ribbons is similar to that obtained previously for similar nanoribbons with evaporated metal electrode contacts [26]. Contrary to the case of nanotubes, whose instrinsic electrical resistance is similar to that of electrode-nanotube contacts, the intrinsic resistance of these MMX ribbons is much higher than that of the contacts. As quasi-one-dimensional conductors, the electrical resistance and the shape of the IV curve of the MMX nanoribbons are mainly dictated by the density of defects in their atomic structure present during the assembly process [25, 26].

With the aim of comparing the electrical contact resistance of EFGs with that of soft-metal electrodes, we also create contacts on these MMX nanoribbons using gold flakes. For this purpose we first evaporate a 30 nm thick film of gold on a glass substrate using a TEM grid as a stencil mask. In this way we obtain 60x60 μm^2 gold squared pads separated by 25 μm. The resulting evaporation is pressed against a viscoelastic polymer to obtain thin gold flakes. Some of the flakes adhering to the polymer are then transferred to a substrate containing MMX nanoribbons, following the same procedure sketched in figure 1. AFM topographic images of the transferred gold flakes show irregular and not abrupt electrode edges, as depicted in figure 3c. Electrical characterization of the MMX nanoribbons (prepared in the same conditions as the ones described above) with these gold flakes contacts is again performed by c-AFM at the same tip-gold electrode distance as in the previous EFG contact, yielding similar resistance (figure 3d).

3.3. Reduced graphene electrical characterization through a double soft-electrode transfer

The next example (summarized in figure 4) consists of a double EGF soft-electrode transfer for electrical characterization of a single layer of reduced graphene oxide. This example illustrates both the possibiblty of creating contacts using 2D materials and the precision achievable when placing the electrodes (another example of the precisión achievable is shown in the supporting information, figure S2, where an iron-cobalt nanoribbon is also made into a contact through double transfer).

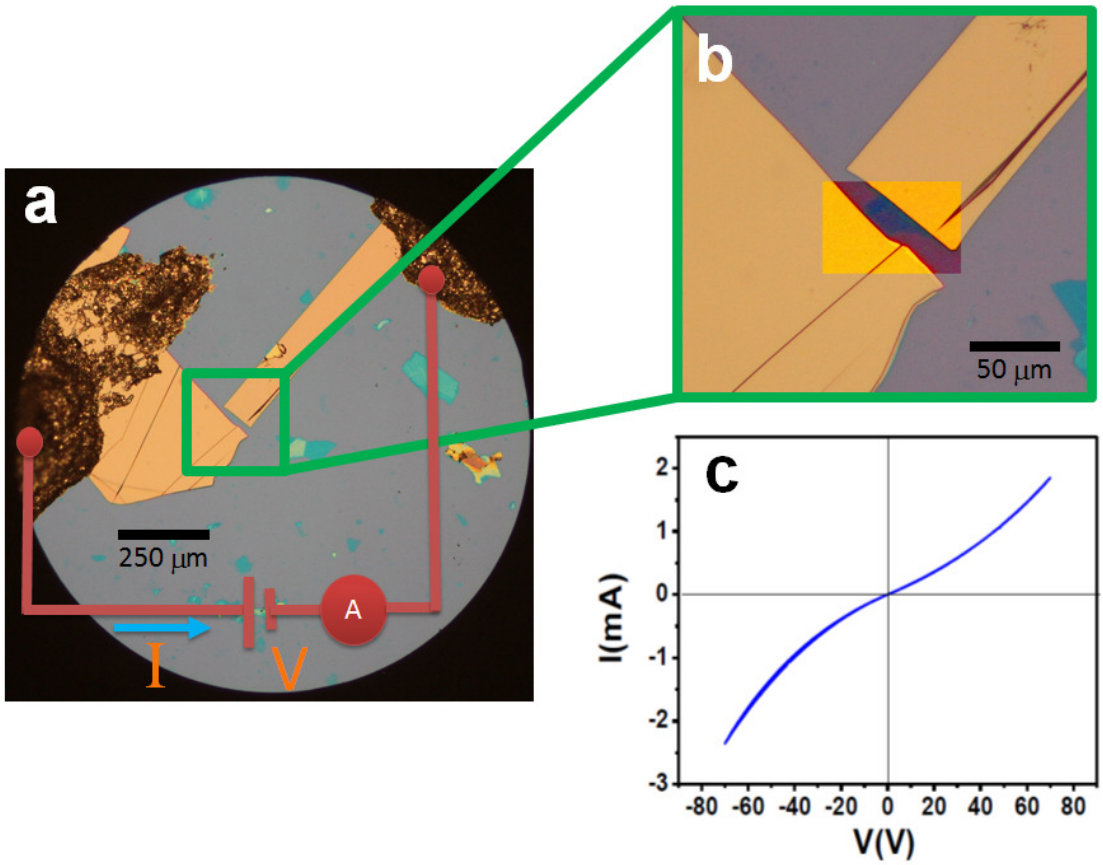

Figure 4. Double electrical contact in graphene oxide (GO) (a) Optical microscope image showing two EGFs with silver paint contacts. The EGFs are in contact with a single layer of graphene oxide. For the sake of clarity a schematic electrical circuit is also included. (b) Zoom-in image of the enclosed region. To allow identification of the GO flake we have increased the contrast in the region of interest. (c) Current versus voltage characteristics of the circuit shown in part (a) after thermal reduction.

Figures 4a and b show two EGF microelectrodes in contact with a graphene oxide (GO) flake. The gap between the two electrodes is ~10 µm. As reported in ref [27], initially the flake is an excellent insulator. The sample is then reduced by annealing it overnight up to 250 ºC in a high vacuum chamber at 10^{-6} mbar [28]. Upon thermal reduction, electrical characterization of the sample is carried out (figure 4c), giving similar results to those found in the literature [27, 28].

3.4. Damaged circuit repair

The last example (figure 5) demonstrates how the controlled transference of EFGs can be used for repairing microcircuits. We illustrate this possibility by repairing two simple microcircuits.

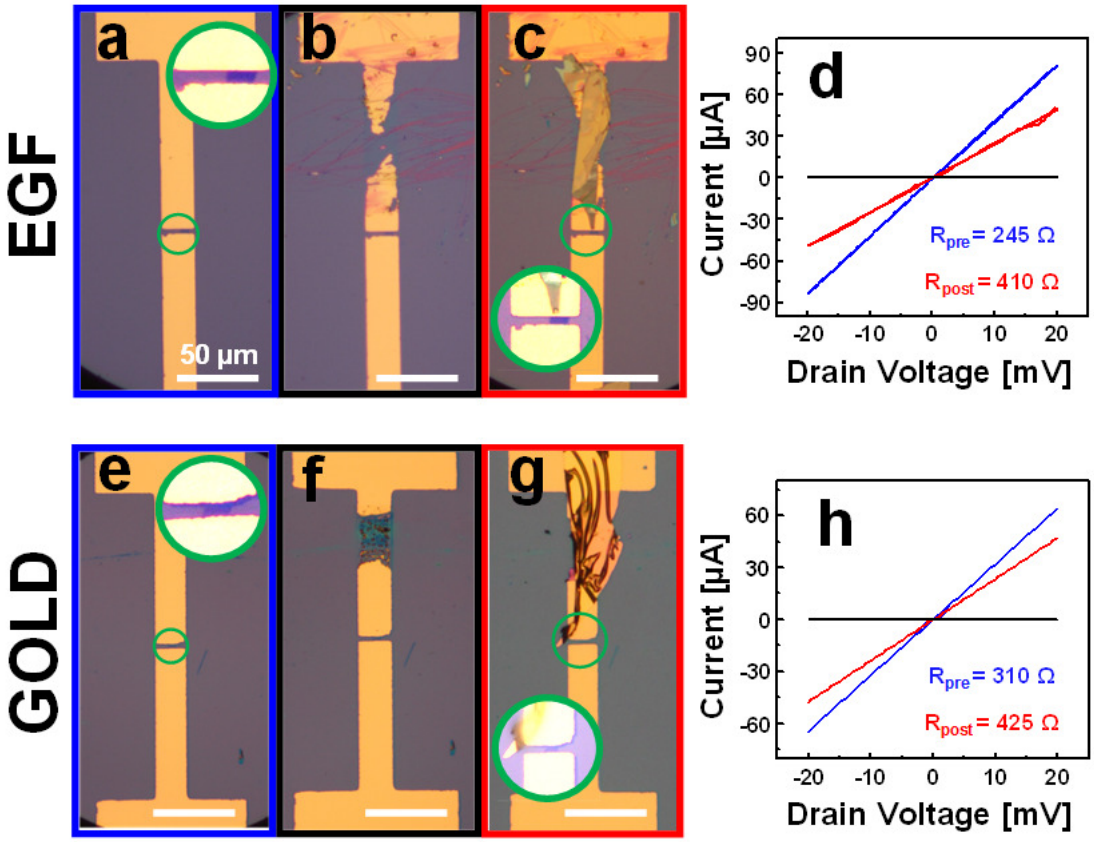

Figure 5. (a) Electrical circuit made by evaporation with a stencil mask. The Au/Cr electrodes are in contact with a pristine bilayer graphene flake. (b) Circuit after being scratched with a tungsten carbide tip. (c) Circuit repaired using an EGF. (d) Current versus voltage characteristics of the intact (blue) and repaired (red) circuit. (e)-(h) The same but now this other circuit was cut using an infrared laser and repaired using a gold thin film. In all cases the insets are zoom-ins of the central regions of the circuits where the graphene flake is placed. Insets in parts c and g show the absence of short-circuits between the upper and lower Au/Cr electrodes.

Figures 5 a-c show a bilayer graphene flake (region enclosed by the circle, see inset) in contact with two Au/Cr electrodes evaporated using a stencil mask. The corresponding current versus voltage characteristic are shown in figure 5d (blue line) where an electrical resistance of 245 Ω is measured. In order to demonstrate the capabilities of soft-electrode transfer, the upper electrode is scratched using a hard tungsten carbide tip, removing part of the metal (figure 5b). The scratched circuit shows an infinite resistance. The circuit is then repaired by transferring an EGF that covers the damaged part. The electrical resistance of the repaired circuit is 410 Ω, (figure 5d). This increase in resistance is probably due to the contact resistance of the EGF flake used to repair the circuit and the gold electrode. Figure 5e portrays a second circuit where a second bilayer graphene flake is in contact with another two Au/Cr electrode pads (region inside the circle, see inset). In this case, the upper Au/Cr electrode is intentionally cut using an infrared

laser (figure 5f). Electrical resistance measurements confirm an open circuit with no current through the damaged pads. To repair this circuit we transfer a 30 nm thick gold film. Figure 5g shows the repaired circuit. Electrical measurements on such repaired circuit show a final resistance of 425 Ω, about a 30% higher than the initial one (figure 5h).
As described in this last example, we observe an increase in resistance in the repaired circuits of a few Ohms. While this resistance is significant for the two cases described here, the vast majority of conducting nano-objects exhibit much higher intrinsic resistances, making this increase in resistance negligible for their electrical characterization. Therefore, the final low resistances obtained after repair validate this methodology.

4. Conclusions

In this report we introduce a simple and inexpensive technique based on the deterministic transfer of soft-electrodes by all-dry viscoelastic stamping. In order to validate and illustrate the uses of this methodology we provide some relevant examples of its many possibilities that include carbon-based materials and metal-organic nanoribbons. The quality of the electrical contacts obtained using this technique is shown to be as good as those obtained by conventional techniques, making this procedure clearly powerful to create contacts with nano-objects. This method is particularly useful in the case of molecules with limited stability under standard lithographic conditions.

Acknowledgements

We want to thank Andres Castellanos for his technical support. This work was supported by Consolider CSD2010-0024, MAD2D-CM, S2013/MIT-3007 and MAT2013-46753-C2-1 and 2.

References

[1] Novoselov K S, Geim A K, Morozov S V, Jiang D, Zhang Y, Dubonos S V, Grigorieva I V and Firsov A A 2004 Electric field effect in atomically thin carbon films *Science* **306** 666-9

[2] Tans S J, Verschueren A R M and Dekker C 1998 Room-temperature transistor based on a single carbon nanotube *Nature* **393** 49-52

[3] Feldman A K, Steigerwald M L, Guo X F and Nuckolls C 2008 Molecular Electronic Devices Based on Single-Walled Carbon Nanotube Electrodes *Acc. Chem. Res.* **41** 1731-41

[4] Holmlin R E, Ismagilov R F, Haag R, Mujica V, Ratner M A, Rampi M A and Whitesides G M 2001 Correlating electron transport and molecular structure in organic thin films *Angewandte Chemie-International Edition* **40** 2316

[5] Nerngchamnong N, Yuan L, Qi D C, Li J, Thompson D and Nijhuis C A 2013 The role of van der Waals forces in the performance of molecular diodes *Nature Nanotech.* **8** 113-8

[6] de Pablo P J, Moreno-Herrero F, Colchero J, Gomez-Herrero J, Herrero P, Baro A M, Ordejon P, Soler J M and Artacho E 2000 Absence of dc-conductivity in lambda-DNA *Phys. Rev. Lett.* **85** 4992-5

[7] Hsu J W P 2005 Soft lithography contacts to organics *Mater. Today* **8** 42-54

[8] Livshits G I, Stern A, Rotem D, Borovok N, Eidelshtein G, Migliore A, Penzo E, Wind S J, Di Felice R, Skourtis S S, Carlos Cuevas J, Gurevich L, Kotlyar A B and Porath D 2014

Long-range charge transport in single G-quadruplex DNA molecules *Nature Nanotech.* **9** 1040-6

[9] Guijarro A, Castillo O, Welte L, Calzolari A, Miguel P J S, Gomez-Garcia C J, Olea D, di Felice R, Gomez-Herrero J and Zamora F 2010 Conductive Nanostructures of MMX Chains *Adv. Funct. Mater.* **20** 1451-7

[10] Cai L T, Tabata H and Kawai T 2000 Self-assembled DNA networks and their electrical conductivity *Appl. Phys. Lett.* **77** 3105-6

[11] Storm A J, van Noort J, de Vries S and Dekker C 2001 Insulating behavior for DNA molecules between nanoelectrodes at the 100 nm length scale *Appl. Phys. Lett.* **79** 3881-3

[12] Meitl M A, Zhu Z T, Kumar V, Lee K J, Feng X, Huang Y Y, Adesida I, Nuzzo R G and Rogers J A 2006 Transfer printing by kinetic control of adhesion to an elastomeric stamp *Nature Mater.* **5** 33-8

[13] Castellanos-Gomez A, Buscema M, van der Zant Herre S J and Steele G A 2014 Deterministic transfer of two-dimensional materials by all-dry viscoelastic stamping. *2D Materials* **1** 011002

[14] Kang J, Shin D, Bae S and Hong B H 2012 Graphene transfer: key for applications *Nanoscale* **4** 5527-37

[15] Wang W, Niu D X, Jiang C R and Yang X J 2014 The conductive properties of single DNA molecules studied by torsion tunneling atomic force microscopy *Nanotechnology* **25** 025707

[16] Burzurí E, Prins F and van der Zant H 2012 Characterization of Nanometer-Spaced Few-Layer Graphene Electrodes *Graphene* **1** 26-9

[17] Tang Q, Tong Y, Li H, Ji Z, Li L, Hu W, Liu Y and Zhu D 2008 High-performance air-stable bipolar field-effect transistors of organic single-crystalline ribbons with an air-gap dielectric *Adv. Mater.* **20** 1511

[18] I. Horcas, R. Fernandez, J. M. Gomez-Rodriguez, J. Colchero, J. Gomez-Herrero and A. M. Baro 2007 WSXM: A software for scanning probe microscopy and a tool for nanotechnology *Rev. Sci. Instrum.* **78** 013705

[19] de Pablo P J, Martinez M T, Colchero J, Gomez-Herrero J, Maser W K, Benito A M, Munoz E and Baro A M 2000 Mechanical and electrical properties of nanosized contacts on single-walled carbon nanotubes *Adv. Mater.* **12** 573-6

[20] Dai H J, Wong E W and Lieber C M 1996 Probing electrical transport in nanomaterials: Conductivity of individual carbon nanotubes *Science* **272** 523-6

[21] de Pablo P J, Gomez-Navarro C, Gil A, Colchero J, Martinez M T, Benito A M, Maser W K, Gomez-Herrero J and Baro A M 2001 Visualization of single-walled carbon nanotubes electrical networks by scanning force microscopy *Appl. Phys. Lett.* **79** 2979-81

[22] Thompson H T, Barroso-Bujans F, Herrero J G, Reifenberger R and Raman A 2013 Subsurface imaging of carbon nanotube networks in polymers with DC-biased multifrequency dynamic atomic force microscopy *Nanotechnology* **24** 12

[23] Dai H J 2002 Carbon nanotubes: opportunities and challenges *Surf. Sci.* **500** 218-41

[24] Gomez-Navarro C, Pablo P J D, Gomez-Herrero J, Biel B, Garcia-Vidal F J, Rubio A and Flores F 2005 Tuning the conductance of single-walled carbon nanotubes by ion irradiation in the Anderson localization regime *Nat Mater* **4** 534

[25] Hermosa C, Vicente Alvarez J, Azani M-R, Gomez-Garcia C J, Fritz M, Soler J M, Gomez-Herrero J, Gomez-Navarro C and Zamora F 2013 Intrinsic electrical conductivity of nanostructured metal-organic polymer chains *Nat. Commun.* **4** 1709

[26] Welte L, Calzolari A, Di Felice R, Zamora F and Gomez-Herrero J 2010 Highly conductive self-assembled nanoribbons of coordination polymers *Nature Nanotech.* **5** 110-5

[27] Gomez-Navarro C, Weitz R T, Bittner A M, Scolari M, Mews A, Burghard M and Kern K 2007 Electronic Transport Properties of Individual Chemically Reduced Graphene Oxide Sheets *Nano Lett.* **7** 3499-503

[28] Jung I, Dikin D A, Piner R D and Ruoff R S 2008 Tunable Electrical Conductivity of Individual Graphene Oxide Sheets Reduced at "Low" Temperatures *Nano Lett.* **8** 4283-7